



Geophysical Research Letters

RESEARCH LETTER

10.1029/2020GL092160

Key Points:

- Nine more TGFs detected by Fermi GBM or Insight-HXMT are found to precede isolated NBEs by a time interval ranging from 60 μs to 13.5 ms
- Seven of these TGFs preceding positive NBEs located at altitudes of 8.6–11 km had harder energy spectrum than EIP-related TGFs
- Relativistic feedback mechanism is probably the mechanism that can explain the production of gammaray photons prior to NBEs

Correspondence to:

G. Lu, gaopenglu@gmail.com

Citation:

Zhang, H., Lu, G., Lyu, F., Xiong, S., Ahmad, M. R., Yi, Q., et al. (2021). On the Terrestrial Gamma-ray Flashes preceding narrow bipolar events. *Geophysical Research Letters*, 48, e2020GL092160. https://doi.org/10.1029/2020GL092160

Received 19 JAN 2021 Accepted 29 MAR 2021

On the Terrestrial Gamma-Ray Flashes Preceding Narrow Bipolar Events

Hongbo Zhang¹ , Gaopeng Lu^{2,3,4} , Fanchao Lyu⁵ , Shaolin Xiong⁶ , Mohd Riduan Ahmad⁷ , Qibin Yi⁶, Dongshuai Li⁸ , Tao Xian² , Jing Yang², Feifan Liu² , Baoyou Zhu² , Yunjiao Pu⁹ , Steven A. Cummer⁹ , Michael S. Briggs¹⁰, and Xiushu Qie^{1,3}

¹Key Laboratory of Middle Atmosphere and Global Environment Observation (LAGEO), Institute of Atmospheric Physics, Chinese Academy of Sciences, Beijing, China, ²School of Earth and Space Sciences, University of Science and Technology of China, Hefei, China, ³Collaborative Innovation Center on Forecast and Evaluation of Meteorological Disasters, Nanjing University of Information Science and Technology, Nanjing, China, ⁴Key Laboratory of Atmospheric Optics, Anhui Institute of Optics and Fine Mechanics, HFIPS, Chinese Academy of Sciences, Hefei, China, ⁵Nanjing Joint Institute for Atmospheric Sciences, Chinese Academy of Meteorological Sciences, Nanjing, China, ⁶Key Laboratory of Particle Astrophysics, Institute of High Energy Physics, Chinese Academy of Sciences, Beijing, China, ⁷Atmospheric and Lightning Research Laboratory, Centre for Telecommunication Research and Innovation (CeTRI), Fakulti Kejuruteraan Elektronik dan Kejuruteraan Komputer, Universiti Teknikal Malaysia Melaka, Melaka, Malaysia, ⁸Instituto de Astrofisica de Andalucía (IAA), CSIC, Granada, Spain, ⁹Electrical and Computer Engineering Department, Duke University, Durham, NC, USA, ¹⁰Center for Space Plasma and Aeronomic Research (CSPAR), University of Alabama in Huntsville, Huntsville, AL, USA

Abstract Narrow bipolar events (NBEs) are occasionally reported to occur within a few ms after Terrestrial Gamma-ray Flashes (TGFs), while the formation mechanism remains mysterious partially due to the lack of sufficient observations. Here, nine more TGFs of this scenario are reported with concurrent LF sferics and lightning location data. The gamma-ray production in these TGFs preceded the occurrence of NBEs by a minimum of $60~\mu s$ up to 13.5~m s, and no other fast leader discharge was found within 20 ms before the TGF. The TGF-preceded positive NBEs occurred at altitudes of 8.6-11~k m in thunderstorms, likely in the high electric field (*E*-field) region of lightning initiation. The analyses show that the NBE-preceding TGFs bear harder energy spectrum with larger proportion of high-energy photons than EIP-related TGFs produced in association with lightning leader. Our findings support the relativistic feedback mechanism of gamma-ray generation in the large-scale thunderstorm *E*-field.

Plain Language Summary Terrestrial Gamma-ray Flashes (TGFs) are brief and intense emissions of hard X-rays and gamma-rays originating inside thunderstorms. Despite the considerable observations confirming the production of high-energy photons during the ascending negative leader typically after the initiation of normal IC lightning (Category-I), there remain some occasional observations indicating that there could be a different scenario for the TGF production, namely the gamma-rays are produced several ms prior to a narrow bipolar event (NBE) (Category-II), which in many cases mark the lightning initiation. In this paper, the TGFs related to NBEs were focused and nine new cases (<4%) were found out of over 230 TGFs with concurrent LF sferics. The comparison between LF sferics and light-curve of gamma-ray emissions corrected with the propagation delay showed that these TGFs clearly preceded the occurrence of NBEs by a minimum of 60 μs up to 13.5 ms. The NBE-followed TGFs typically endured longer by containing more gamma-ray photons and the energy spectrum was usually harder than Category-I TGFs whose generation involves the progression of an energetic lightning leader. The TGFs observed preceding the lightning initiation in this study generally support the relativistic feedback mechanism for the generation of TGFs in the large-scale thunderstorm *E*-field.

1. Introduction

Terrestrial Gamma-ray Flashes (TGFs) are brief high-energy emissions of photons discovered unexpectedly by the Burst and Transient Source Experiment (BATSE) (Fishman et al., 1994), manifesting the most energetic photon emissions due to the bremsstrahlung radiation of electrons forged in tropospheric thunderstorms. The photon energy of TGFs typically exceeds 1 MeV or even over 40 MeV (Marisaldi et al., 2010;

© 2021. American Geophysical Union. All Rights Reserved.

ZHANG ET AL. 1 of 12



Smith et al., 2005). The analyses of lightning mapping observations related to TGFs detected by space-borne platforms, such as the Reuven Ramaty High Energy Solar Spectroscopic Imager (RHESSI) and the Gamma-ray Burst Monitor (GBM) on the Fermi Gamma-ray Space Telescope (Briggs et al., 2010; Smith et al., 2005), attribute the gamma-ray production to the upward progression of initial negative leader after the inception of ordinary intra-cloud (IC) lightning (Lu et al., 2010; Lyu et al., 2018). This scenario (Category-I, hereinafter) is consistent with several features exhibited by most TGF-associated radio-frequency lightning signals, including the presence of a fast impulse marking lightning onset, a major impulse directly linked to gamma-ray production (Cummer et al., 2011; Neubert et al., 2020; Østgaard et al., 2013), and often a considerable charge moment change as indicated by the measurement of ultra-low-frequency magnetic pulse (Cummer et al., 2005; Lu et al., 2011, 2019) and close electric field (*E*-field) change (Marshall et al., 2013). The majority of TGFs were associated with a type of energetic LF pulses, which is now usually referred to as the energetic in-cloud pulse (EIP) (Lyu et al., 2015, 2016). Besides, downward TGFs were also observed at ground level (Belz et al., 2020; Dwyer et al., 2004; Hare et al., 2016; Tran et al., 2015), substantially expending the understanding on the highly energetic radiation phenomena of lightning.

Despite the considerable observations confirming the gamma-ray production during the ascending negative leader after the initiation of IC lightning, there were some exceptional observations, occasionally, indicating that there could be a second scenario (Category-II, hereinafter) for TGF production, namely the gamma-rays are produced a few ms prior to lightning initiation (e.g., Shao et al., 2010; Stanley et al., 2006), which is usually marked by the occurrence of a special type of IC discharge called narrow bipolar event (NBE) or compact intra-cloud discharge (CID) with compact size and strong very-high frequency (VHF) radiation (Leal & Rakov, 2019; Nag et al., 2010; Smith et al., 2004; Tilles et al., 2020; Zhang et al., 2016). Shao et al. (2010) suggested that the NBE occurrence could be preconditioned by the TGF-producing process. Recently, Lu et al. (2019) reported a TGF composed of three individual pulses preceding the associated NBE by approximately 4 ms. These observations entangle the understanding on the physical connection between lightning and gamma-ray production, and more observations are desired to understand the relationship between NBEs and TGFs.

In this paper, we focus the analyses on totally nine new observations of NBEs following TGFs (i.e., Category-II) mostly produced by tropical thunderstorms. These NBEs were measured at range of 150 –2,200 km by the low-frequency (LF) magnetic sferics recording site. In addition to eight TGFs detected by Fermi GBM (Briggs et al., 2010), our data set also includes one TGF event registered by the *Insight*-Hard X-ray Monitor Telescope (*Insight*-HXMT) as the first X-ray astronomy satellite of China (Zhang et al., 2020b).

2. Measurements and Data

The concurrent broadband lightning sferics are critical to understand the physical connection between TGF and lightning (e.g., Cummer et al., 2005; Lu et al., 2010, 2011; Shao et al., 2010). Since summer of 2014, we have been building a network of low-frequency (10–400 kHz, LF) magnetic sensors (with two orthogonal induction coils) to record lightning signals related to TGFs detected by various platforms. The LF signals are continuously recorded at 1 MHz (with time accuracy better than 1 μ s). At present, this network consists of 12 stations in China and one oversea station on the campus of Universiti Teknikal Malaysia Melaka (UTeM), Malaysia (Sabri et al., 2019; Zhang et al., 2020a), as part of the Lightning Effects Research Platform (LERP) (Huang et al., 2018). The LF data examined in this work were acquired respectively at MALA station (2.314°N, 102.318°E), XIAM station (24.625°N, 118.081°E), CONG station (23.639°N, 113.596°E) and LHAS station (30.063°N, 90.315°E) as shown in Figure 1a.

In addition to TGFs detected by Fermi GBM orbiting at \sim 560 km altitude with an inclination of 25.6° (Briggs et al., 2010), we also examined TGF detections of *Insight*-HXMT launched in June of 2017 (Zhang et al., 2020b). *Insight*-HXMT orbits around the Earth at 550 km altitude with inclination angle of 43° (Lu et al., 2020); our analyses refer to the High-Energy X-ray module of *Insight*-HXMT, which contains 18 NaI/CsI detectors covering the energy range of 20–250 keV for pointing and scanning observation and the energy range of 0.2–3 MeV for the all-sky gamma-ray monitoring (Zhang et al., 2020b). Figure 1a shows the distribution of subsatellite points upon the TGF detections of *Insight*-HXMT (blue "+"s) and Fermi (gray "×"s), respectively, from July of 2017 to April of 2020.

ZHANG ET AL. 2 of 12

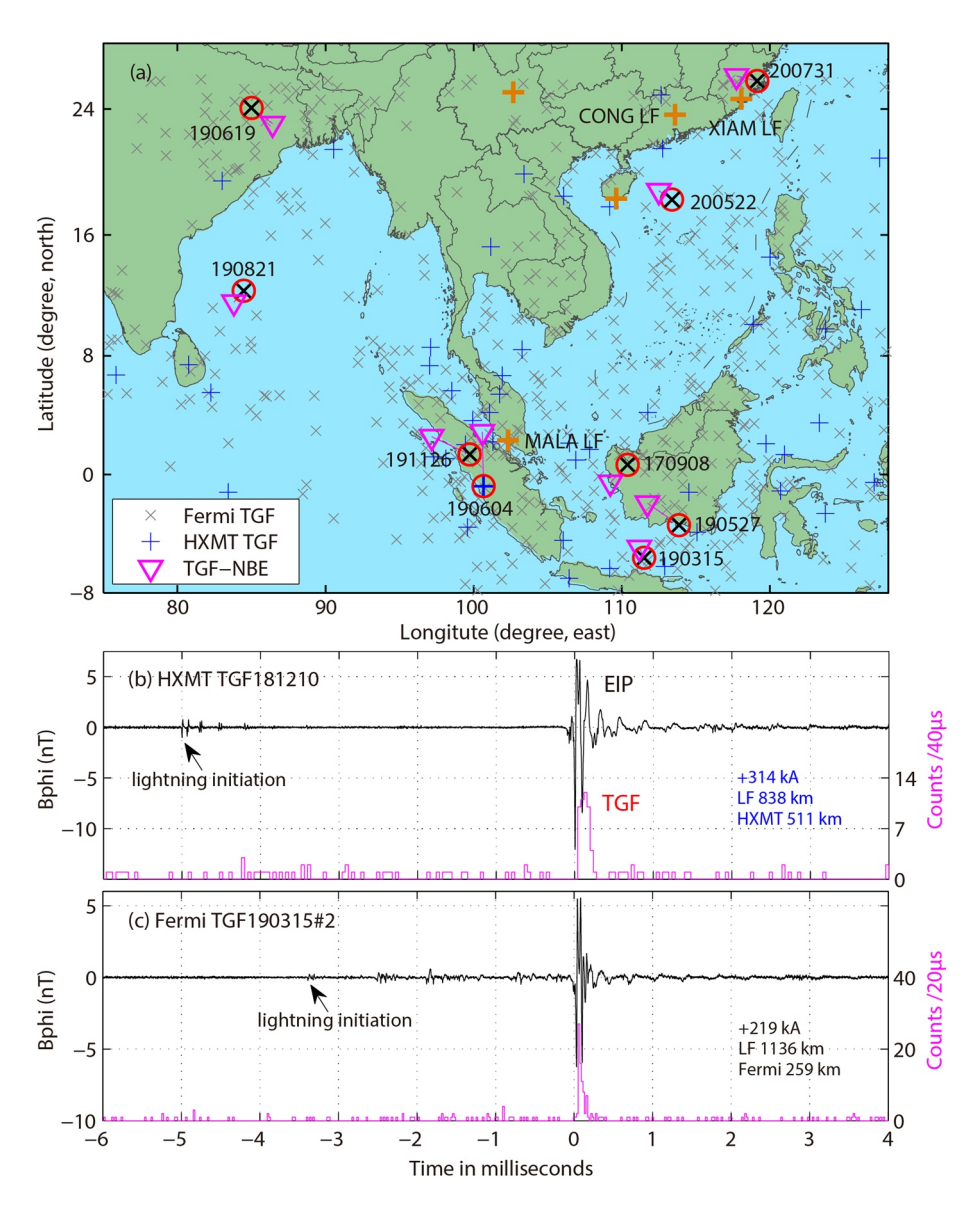


Figure 1. (a) Schematic diagram of TGF observations by *Insight*-HXMT (blue "+"s) and Fermi (gray "×"s) during July 2017 to April 2020. The footprints and lightning locations of nine NBE-related TGFs (Category-II) were marked by red " \otimes "s and pink " ∇ "s, respectively. (b) Time-corrected photon data (pink lines) and the corresponding LF sferics (one energetic in-cloud pulse, EIP. black lines) of TGF181210 detected by *Insight*-HXMT, illustrating the timing of using data is accurate. (c) Same with (b), but for a TGF detected by Fermi that was also associated with an EIP.

Since 2016, the associated lightning signals have been recorded at one or more LERP stations for over 200 TGFs, including 12 events from *Insight*-HXMT detections. For these TGFs, we first searched for the TGF-associated lightning signal from the LF data recorded at the closet LERP station, with a maximum 50 ms temporal offset from the TGF detection (e.g., Cummer et al., 2005). Then, when the lightning signal is identified, we searched for the lightning discharge from Vaisala's Global Lightning Data set (GLD360, providing time, location, peak current and type of lightning discharges) (Mallick et al., 2014) with a maximum lateral displacement of 800 km from the satellite footprint (e.g., Connaughton et al., 2010), and examined the TGF-associated sferics in comparison with the light-curve of gamma-ray emissions when both are subtracted by the propagation delay. It is assumed that the source altitude of TGFs was at 12 km (e.g., Cummer et al., 2014).

Figures 1b and 1c show two examples of Category-I TGFs that were detected by *Insight*-HXMT and Fermi GBM, respectively. Both TGFs were associated with EIPs detected by GLD360 with high peak current

ZHANG ET AL. 3 of 12



(+314 kA and +219 kA, respectively). As shown in the figure, for these two TGFs, the LF signal and light-curve of gamma-rays are almost simultaneous, confirming that the time accuracy of *Insight*-HXMT TGF detection is better than 100 μ s (Li et al., 2018).

Eventually, nine TGFs (eight by Fermi GBM and one by *Insight*-HXMT, red " \otimes "s shown in Figure 1a) were identified as Category-II events by preceding an NBE-type IC discharge (pink " ∇ "s) that was selected with the criteria similar to previous studies (e.g., Wu et al., 2012, 2013; Zhang et al., 2016). It is also confirmed that there was no other fast discharge within 20 ms before the TGF based on the recorded LF signal. The distance between satellite footprint and NBE location (given by GLD360 for the first eight cases and inferred from the sferic bearing and radar reflectivity for the last case) ranges from 85 to 410 km and the zenith angle is estimated to range from 9.0° to 36.7°, in line with the typical values (\sim 30–40°) given by Gjesteland et al. (2011).

3. Case Studies and Results

The concurrent LF signals and photon light-curve are plotted in Figure 2 for the nine Category-II TGFs, showing that for the first eight cases (Figures 2a-2h), the gamma-ray pulse clearly preceded the NBE by 1.2 –13.5 ms; for the last case TGF200522 (Figure 2i), the gamma-ray pulse and NBE discharge were almost simultaneous, whereas the onset of gamma-ray pulse appears to precede the NBE by 60 µs. Among these TGFs, seven cases (Figures 2a-2d and 2f-2h) were related with positive NBEs (with downward current) whose height was estimated to be 8.6-11 km (above mean sea level, MSL), slightly lower than the typical altitudes (about 12 km) of EIPs associated with Category-I TGFs (e.g., Cummer et al., 2014; Lu et al., 2010) and positive NBEs (e.g., Smith et al., 2004; Wu et al., 2012; Zhang et al., 2016), while roughly higher than positive NBEs initiating lightning flashes (INBEs) (Wu et al., 2014). They were all almost located in the center of strong convection of thunderstorms with the closest black body temperature (TBB) of 192-201 K given by the Chinese geostationary satellite Fengyun-2G with 1-h temporal resolution and 5-km spatial resolution (www.nsmc.org.cn). However, the other two TGFs (Figures 2e and 2i) were related to negative NBEs usually with higher altitudes (Liu et al., 2018; Wu et al., 2014) and the source height of TGF200522 was estimated to be about 20 km. The two TGFs exhibited different features: TGF190821 was near the edge of convection with TBB <228 K, while TGF200522 was at the center of stronger convection with TBB of 182 K, coldest among all the nine TGFs.

The common feature of these TGFs suggests that Category-II TGFs were probably produced by the thunderstorm E-field as suggested by Dwyer (2008), other than the strong E-field formed by the upward negative leader (e.g., Mailyan et al., 2019; Xu et al., 2015). Note that the TGF shown in Figure 2c was detected by Fermi GBM only 5 s after the observation of the Category-I TGF shown in Figure 1c, whereas these two TGFs appeared to originate from two different thunderstorm cells about 172 km apart.

In the following, we examine two cases (Figures 2a and 2b) in details that were detected by *Insight-HXMT* and Fermi GBM, respectively. For these two events, the TGF-preceded NBE signal was measured at a relatively close distance and contained clear ionospheric reflection necessary for determining the source height.

3.1. TGF Case on June 4, 2019

At 2111:31.671 UTC on June 4, 2019, *Insight*-HXMT detected a TGF when the footprint was at $(0.796^{\circ}S, 100.673^{\circ}E)$. The TGF light-curve contained 29 gamma-ray photons over 364 μ s. As indicated by the LF signal (Figure 3b) recorded at MALA station, the gamma-ray production preceded a sequence of NBEs (marked as NBE1, NBE2, and NBE3 in the figure). The first NBE (NBE1) was registered by GLD360 as an IC event at $(2.886^{\circ}N, 100.587^{\circ}E, red "V" in Figure 3a)$ with +27 kA peak current (lightning type was confirmed by the recorded LF wave signals. There may be some error in the reported current, while it could reflect the relative magnitude of NBEs). As shown in Figure 3a, NBE1 was about 410 km from the *Insight*-HXMT footprint and 202.6 km from MALA station, and it was located in the strong convection of a mature-stage thunderstorm. With the ionospheric reflection signals clearly identified for NBE1 (see the inset of Figure 3b), we apply the method of Zhang et al. (2016) to estimate the height of NBE and ionospheric reflection to be 10.5 km (MSL) and 96 km, respectively.

ZHANG ET AL. 4 of 12

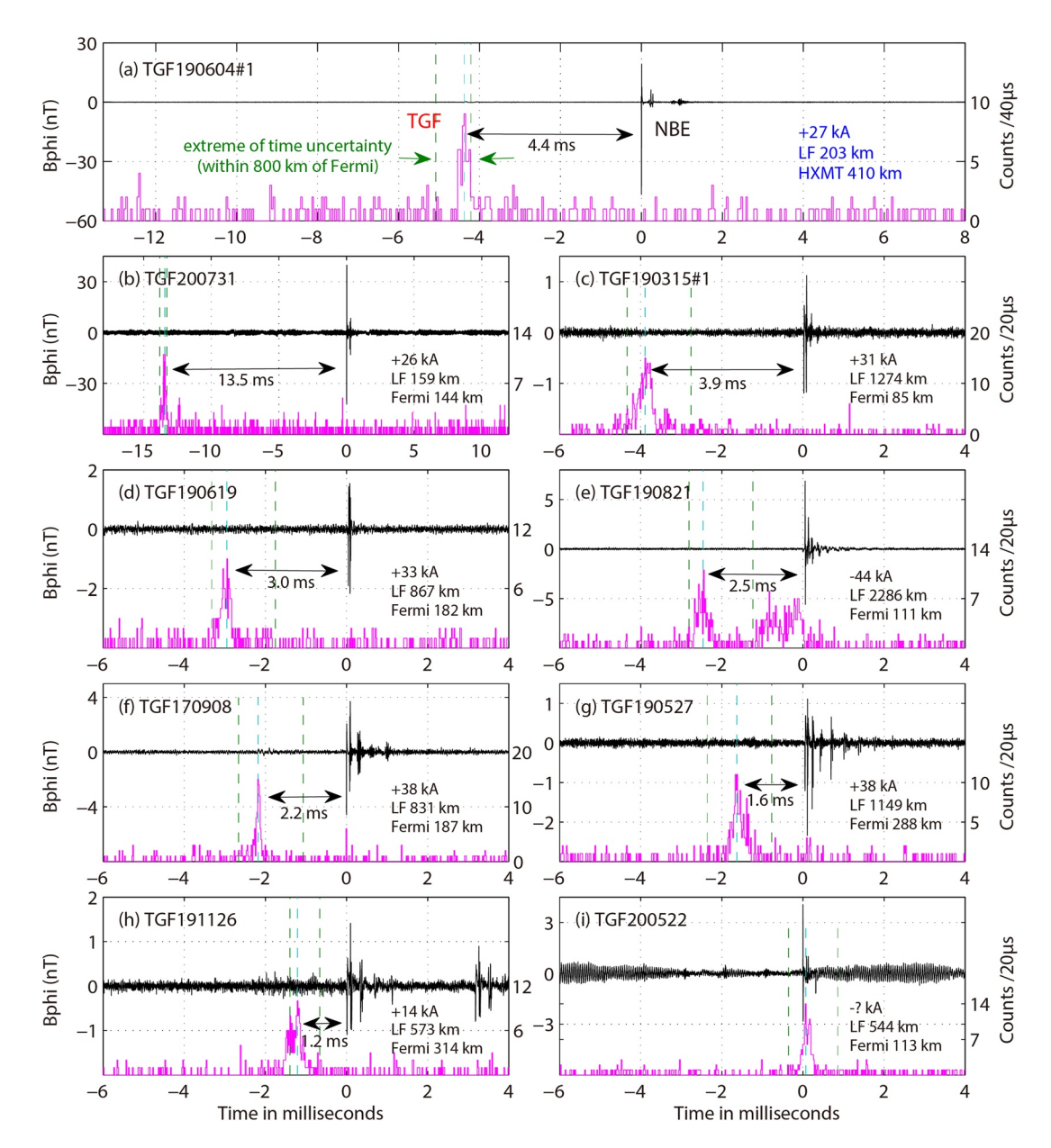


Figure 2. Light-curve of gamma-ray emissions (pink lines) and the corresponding LF sferics (black lines) of NBEs for nine Category-II TGFs analyzed in this paper. The propagation delay is corrected by presuming that the gamma-ray production is at 12 km (MSL) near the NBEs. TGF190604#1 was detected by Insight-HXMT (a), while other eight TGFs were by Fermi GBM (b)–(g). The time intervals between TGF and NBE, and the extreme of time uncertainty when the TGF source was at any position within 800 km of Fermi were marked as cyan and green lines, respectively. The distance of TGF footprint-lightning location and LF station-lightning location, the pulse peak current with polarity are shown in each panel. (The NBE related to TGF200522 was not located by GLD360 and the current was unknown. Instead, one GLD360-registered fast discharge (about 9.5 ms later) from the similar bearing was used as the source location of TGF).

The second NBE (NBE2) was also located by GLD360 (with peak current of \pm 18 kA) at a similar location; the third NBE (NBE3) was not detected, but it probably occurred in the same thundercloud with similar bearing to the earlier NBEs. In fact, within 750 ms after the TGF of our interest, over 20 magnetic deflections can be identified from the LF signal and most of them were NBEs; two more NBEs were detected by GLD360 in the same thunderstorm, and most of the others were from the same direction. Almost all NBEs with discernible ionospheric reflections were determined to occur at heights above NBE1, but with much smaller amplitude.

ZHANG ET AL. 5 of 12

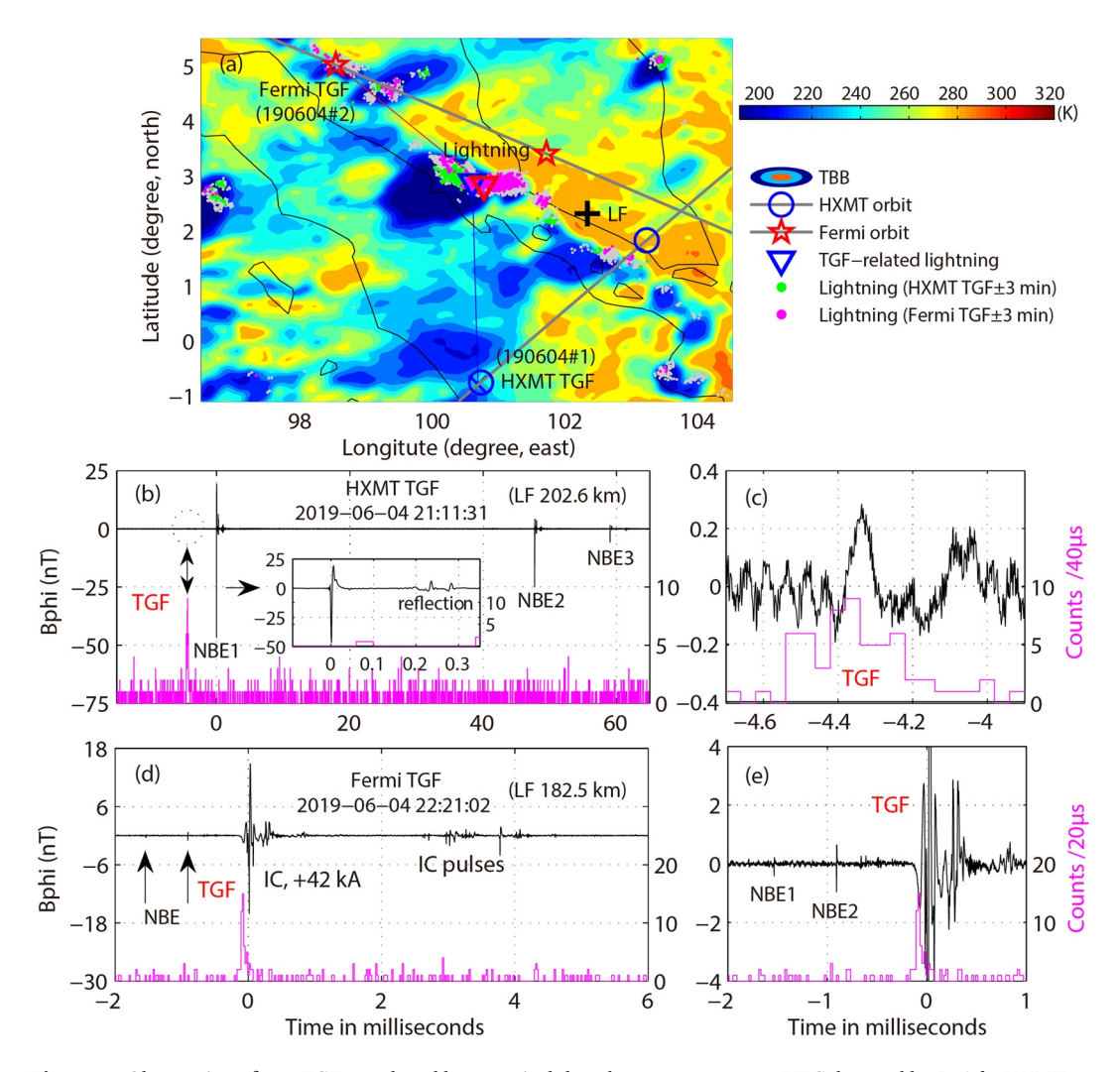


Figure 3. Observation of two TGFs produced by a tropical thunderstorm at 2111:31 UTC detected by *Insight*-HXMT (referred to TGF190604#1) and 2221:02 UTC by Fermi GBM (TGF10604#2), respectively. (a) The footprint (blue "○") and related NBE location (red "∇") of *Insight*-HXMT TGF190604#1, overlapping on the closest FY-2G TBB data at 2200 UTC on June 4, 2019. The footprint (pink "☆") and related IC discharge location (blue "∇") of TGF190604#2 were shown. The lightning occurred near the two TGFs were marked as green and pink points. (b) TGF190604#1: Time-corrected photon data and related lightning sferics measured by MALA LF station (202.6 km away). The inset is the expended view of TGF-related NBE1 with clear ionosphere reflection. (c) Part of (b): 1 ms of LF data associated with the pulse of TGF light-curve. (d) Same as (b), but for TGF190604#2 (182.5 km away). (e) Part of (d) same as (c), but for TGF190604#2 in 3-ms window.

The GLD360-registered NBEs were confined within a 5 \times 5 km thundercloud region with strong convection. By presuming that the TGF examined was produced in this region, it is inferred that the gamma-ray production preceded NBE1 by about 4.4 ms (Figure 3b). The TBB of this region as given by FY-2G was about 191 K, much colder than that (234 K) inferred for a Category-I TGF examined previously (Zhang et al., 2020a), whose source height was also estimated to be around 10.5 km (MSL). Therefore, the thunderstorm hosting the Category-II TGF examined in this section appeared to develop a relatively deep convection, and the gamma-rays are expected to travel over a relatively long path in the thundercloud.

Interestingly, as zoomed in Figure 3c, there was a weak magnetic pulse with duration of about 200 μ s that is almost synchronized with gamma-ray production. The signals of two orthogonal coils indicated that the pulse was from the same direction as the following NBE. The slow pulse exhibits similar feature to previous studies (Cummer et al., 2011; Pu et al., 2019), who attributed the main TGF-associated LF pulse to the electron acceleration during TGF production. A similar slow pulse was associated with TGF170908 (Figure 2f),

ZHANG ET AL. 6 of 12



while no similar pulse was found in other seven cases. However, there is also some difference between them: the slow pulse of our Category-II TGF occurred 4.4 ms before a sequence of NBEs, rather than during a sequence of fast leader discharges. The temporal relationship between TGF and NBE (without synchronous or close leader discharges) implies that the gamma-ray production by the thunderstorm *E*-field could also make conditions favorable for the occurrence of NBEs.

It is also noticed that, about one hour later, Fermi GBM following a different path detected another TGF at 2221:02.132 UTC over (5.074°N, 98.478°E) from the same thunderstorm as TGF190604#1. This TGF (referred to TGF190604#2) appeared brighter by containing 55 gamma-ray photons over 320 μ s. As shown in Figure 3a, the TGF-related lightning located by GLD360 at (2.838°N, 100.761°E) was about 354 km from Fermi footprint and 182.5 km from MALA station, also in the convection region that moved eastward and still was at the mature stage. As shown in Figures 3d and 3e, the gamma-ray pulse corresponded to an EIP-like IC discharge (namely Category-I) with +42 kA peak current detected by GLD360, which was the strongest pulse of the parent IC. The estimated height of this pulse was about 11.0 km (Figure 3e), slightly higher than the previous Category-II TGF190604#1.

3.2. TGF Case on July 31, 2020

The second Category-II TGF examined was detected by Fermi GBM at 1155:37.588 UTC on July 31, 2020, when the Fermi footprint was at $(25.725^{\circ}N, 119.151^{\circ}E)$ near XIAM station. The light-curve contained 142 photons over 650 μ s. Figure 4a shows the GLD360 lightning events (magenta points) within 1-h interval centered at this TGF as superimposed on the Fengyun-2G TBB data at 1200 UTC. The distinct NBE (at 1155:37.673 UTC) preceded by this TGF was detected by GLD360 with peak current of +26 kA at $(26.025^{\circ}N, 117.749^{\circ}E)$ (pink "V"), about 144 km from Fermi footprint and 159 km from XIAM station. The TBB and S-band weather radar data showed that the TGF-preceded NBE occurred in the convection region of a mesoscale convective system, almost in the coldest region (the area below 220 K was about 36,431 km² including convection and stratiform region acquired from radar data) that was at the later stage of maturity.

As shown in Figure 4c, with time shifted back to the source region, the lightning pulse occurred about 13.5 ms after the gamma-ray production. The height of this NBE was estimated to be 9.8 km (MSL). There were also several small NBE-like IC pulses after the major NBE (while they did not constitute a typical full-fledged IC), but the ionospheric reflections are not discriminable (probably due to a relatively close distance). However, even the distance is closer than the Category-II TGF examined in Section 3.1, there was no discernible pulse that appear to accompany the gamma-ray production (Figure 4d).

4. Discussions

At present, two types of mechanisms have been proposed to explain the gamma-ray production associated with electrified thunderstorms, i.e., the relativistic feedback model (e.g., Dwyer et al., 2012) and the lightning leader-seeded model (e.g., Celestin et al., 2012; Xu et al., 2012). The latter requires a lightning leader to generate the high *E*-field region and the gamma-ray production usually corresponds to a fast leader discharge, which appear to be mostly observed scenario from the perspective of space-borne platforms.

For the former model, it requires a large-scale E-field to drive the acceleration of electrons, while the high E-field at the tip of leader is not necessary. As examined in Section 3, the gamma-ray burst of eight TGFs examined in this paper all preceded the NBE by 1.2 –13.5 ms; there were no fast leader discharges within 20 ms prior to the TGF. The common feature exhibited by these Category-II TGFs is consistent with gamma-ray production in the large-scale thundercloud E-field rather than by the leader process, as proposed in the relativistic feedback mechanism.

Previous studies showed that Category-I TGFs occurred typically several ms after the lightning onset (which sometimes is marked by an NBE) when the initial upward negative leader has ascended for 1–3 km (Cummer et al., 2014; Lu et al., 2010; Zhang et al., 2020a). For Category-II TGFs, especially those related to positive NBEs, the high-energy photons are likely produced in the vicinity of lightning initiation deeper in thunderstorms, without invoking the participation of any fast discharges in the TGF production. Hence, when TGFs of both categories are detected by satellites, the energy spectrum of Category-II TGFs should

ZHANG ET AL. 7 of 12

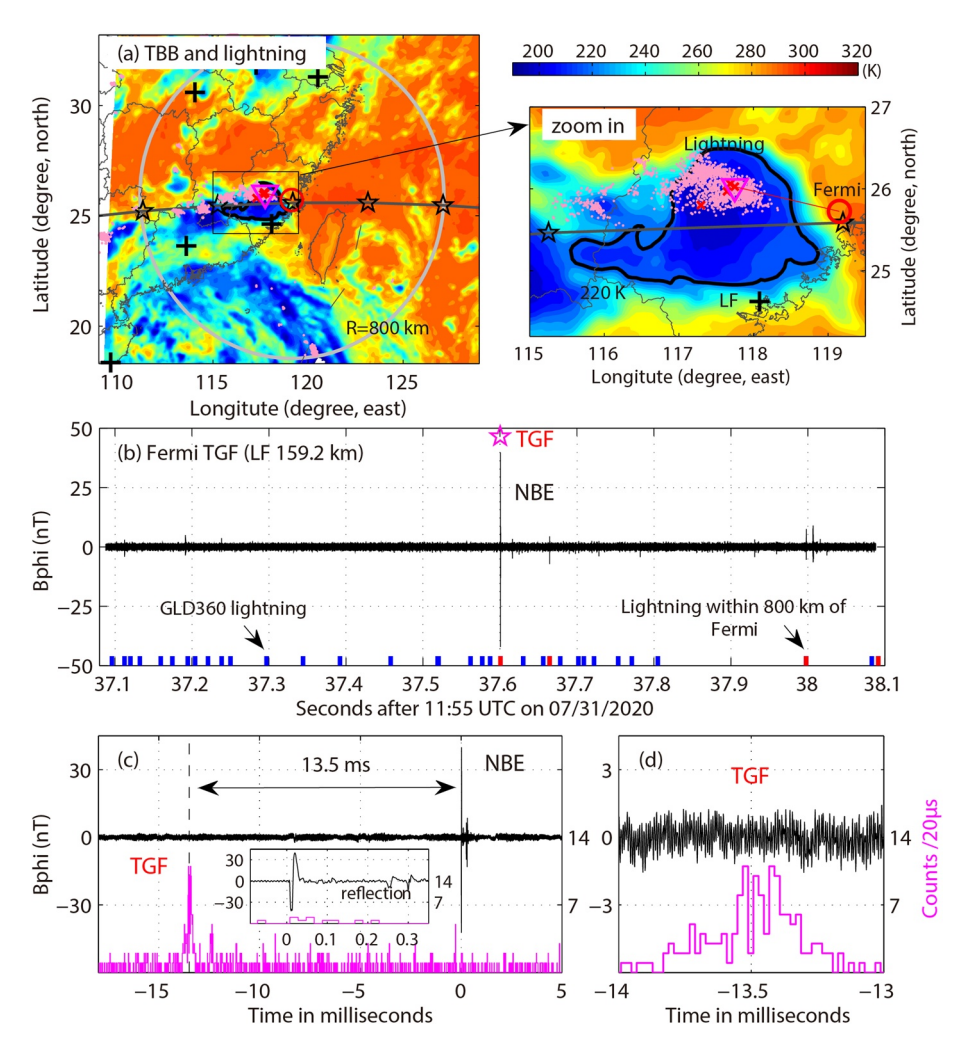


Figure 4. Observation of one TGF detected by Fermi at 1155:37 UTC on July 31, 2020. (a) FY-2G TBB data at 1200 UTC superposed with the footprint ("☆") and related lightning location ("V") of TGF200731, all lightning discharges (magenta points) between 1125 and 1225 UTC and the four lightning discharges within 1 s and 800 km of Fermi (short red lines in (b)). The radius of gray circle is 800 km centered at TGF footprint. Right is the enlarged view. (b) 1-s LF sferics related to TGF200731 overlapped with all lightning (short blue lines) and four lightning occurred within 800 km of Fermi (red lines). (c) Time-corrected photon data and the related lightning sferics measured at XIAM station (159.2 km away) in 23 ms window. The inset is the expended view of TGF-related NBE with clear ionosphere reflection. (d) Part of (c) 1 ms of LF data associated with the light-curve pulse.

be harder than that of Category-I TGFs. Two Fermi GBM TGFs of Category-II noticed previously, including one examined by Lu et al. (2019), are combined with the nine events studied in this paper for an analysis on a statistical basis. As shown in Figures 5c-5e, Category-II TGFs detected by Fermi contained more photons and endured longer (blue color), while the photon counts per μs were less than 17 Category-I TGFs (black color). The magnitude for the peak current of NBEs preceded by Category-II TGFs ranges from 14 to 44 kA, much smaller than that of EIPs associated with Category-I TGFs (Figure 5f). Figure 5g shows that Category-II TGFs contained more gamma-ray photons with energy >800 keV than Category-I TGFs from the 12 NaI detectors on Fermi GBM; similarly, Category-II TGFs have a higher ratio between photons registered by BGO detectors and NaI detectors, respectively. Figures 5a and 5b show the average (and standard deviation) energy spectrum of two categories from the NaI detection and the BGO detection, respectively. Again, we can see that Category-II TGFs contained more photons with higher energy, namely they were "harder" than Category-I TGFs. It is consistent with the speculation that Category-II TGFs related to positive NBEs typically occur at a relatively low altitude than Category-I TGFs associated with an upward negative leader. The characteristics and energy spectrum of TGF200522 related to a negative NBE (Figure 2i) was similar to other

ZHANG ET AL. 8 of 12

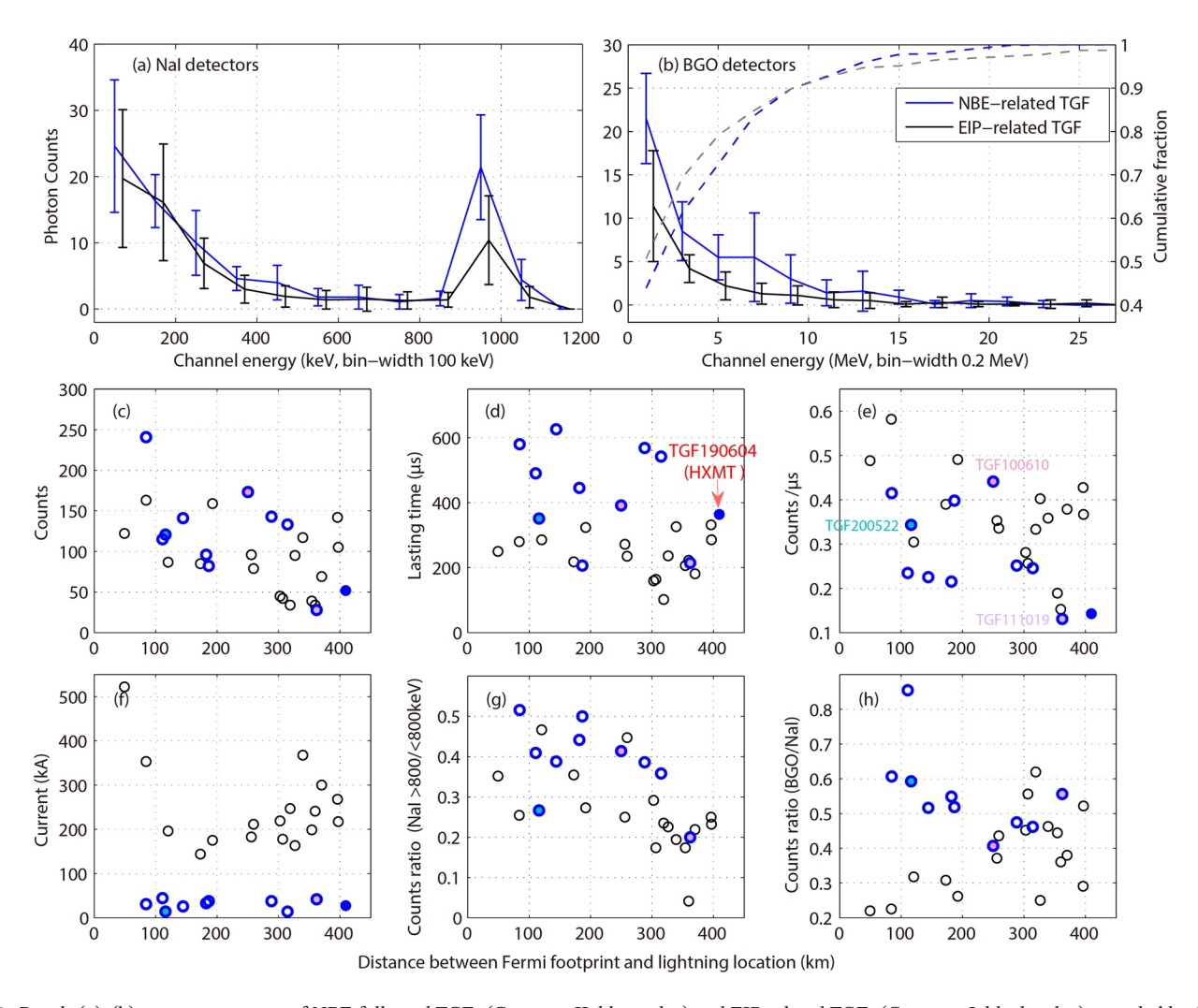


Figure 5. Panels (a), (b): energy spectrum of NBE-followed TGFs (Category-II, blue color) and EIP-related TGFs (Category-I, black color) recorded by 12 NaI detectors (panel a) and two BGO detectors (panel b). Panels (c)–(f): photon counts, lasting time, photon counts per microsecond and peak current of both categories of TGFs. Panel (g): ratio between the photon counts with energy greater and lower than 800 keV as recorded by NaI detectors. Panel (h): photon counts ratio of BGO detectors to NaI detectors. NBE-followed TGFs (produced by the thunderstorm) exhibit different features from EIP-related TGFs (produced by the lightning leader).

eight cases, indicating that the gamma-ray pulse and NBE could be produced by the large-scale thunder-cloud E-field in a short time or simultaneously; while the TGF may also be produced directly by a negative NBE. That is, the TGFs preceding NBEs of different polarities could be produced via different mechanisms, which needs more observations to clarify.

Category-II TGFs preceded the NBE by up to 13.5 ms, and there is no confirmed evidence for the occurrence of leader-related fast discharge after the TGF-preceded NBE. We analyzed all the TGFs with LF signals of high signal-to-noise ratio (SNR > 10) and GLD360 lightning location within time window [1, 10] ms after the TGF. Eventually, 26 TGFs were found in addition to Category-II TGFs examined in this paper. Based on the location information, the time-corrected LF signals and photon light-curve indicate that these 26 TGFs either corresponded to a fast IC discharge missed by GLD360 (in 24 cases), or occurred during the initial stage of IC lightning without a corresponding fast discharge (in two cases simultaneous to a slow pulse like that of Pu et al. (2019)). There was also one TGF that occurred during a sequence of NBEs. The analyses above confirm that the NBE-followed TGFs are a special category of TGFs without invoking the existence of lightning leader. Category-II TGFs are likely produced by the large-scale high thunderstorm E-field, which is also capable of producing NBEs, and the gamma-ray production might even create a favorable condition for the occurrence of NBEs.

ZHANG ET AL. 9 of 12



5. Conclusions

Previous studies have mainly focused on TGFs that appear to be produced during the initial upward leader progression after the lightning inception, which is sometimes marked by the occurrence of a narrow bipolar event (NBE). There are also occasional reports of TGFs that precede an NBE by a few ms, but the associated mechanism remains mysterious partly due to lack of sufficient observations. In this paper, we present the observations of seven more TGFs showing that the gamma-ray production precedes the occurrence of a positive NBE by a short time ranging 1.2 –13.5 ms. The altitude of TGF-preceded NBEs was estimated to range from 8.6 to 11 km. Our data set includes one TGF detected by the Chinese Hard X-ray Modulation Telescope (*Insight*-HXMT). Interestingly, for this TGF, our LF station likely recorded the signal directly associated with gamma-ray production; moreover, about 70 min later, the Fermi GBM observed an EIP-like-associated TGF produced in the same thunderstorm. Detection of multiple TGFs from the identical thunderstorm has also been reported previously by Ursi et al. (2016). Besides, we noticed two even rarer cases of TGFs associated with negative NBEs: in the first case, the gamma-ray production appeared to initiate 2.5 ms before and became terminated by the NBE; in the second case, the TGF was almost simultaneous to the NBE, whereas the onset of gamma-ray production slightly preceded the discharge.

Our analyses on a statistical basis indicate that the NBE-related TGFs had a harder energy spectrum with larger proportion of higher-energy photons and they are expected to occur near the location of lightning initiation at a relatively low altitude in parent thunderstorms. The results indicated that the NBE-related TGFs were produced by the large-scale thunderstorm E-field, supporting the relativistic feedback mechanism of TGF generation. That is, the high E-field between the two major charge layers in the thundercloud is also capable of producing TGFs, and the TGF-producing process could even further contribute to generate NBEs (e.g., Shao et al., 2010).

Data Availability Statement

The TGF data are available at online archives as follows: FERMI (https://heasarc.gsfc.nasa.gov/FTP/fermi/data/gbm/daily/) and *Insight*-HXMT (www.hxmt.org). Thanks to Vaisala Inc. for providing the GLD360 data (https://www.vaisala.com/en/products/systems/lightning/gld360). The data used for this analysis are available on the data repository website (https://zenodo.org/record/4584660#.YETldVwzaUk).

Acknowledgments

This work was supported by the National Key R&D Program of China (2017YFC1501501), National Natural Science Foundation of China (U1938115, 41805004, and 41875006), and the Chinese Meridian Project. The *Insight*-HXMT mission is a project funded by China National Space Administration (CNSA) and Chinese Academy of Sciences (CAS). The Fengyun-2G satellite images are provided by National Satellite Meteorological Center (NSMC) of China (www.nsmc.org.cn).

References

- Belz, J. W., Krehbiel, P. R., Remington, J., Stanley, M. A., Abbasi, R. U., LeVon, R., et al. (2020). Observations of the origin of downward terrestrial gamma-ray flashes. *Journal of Geophysical Research: Atmospheres*, 125, e2019JD031940. https://doi.org/10.1029/2019JD031940
 Briggs, M. S., Fishman, G. J., Connaughton, V., Bhat, P. N., Paciesas, W. S., Preece, R. D., et al. (2010). First results on terrestrial gamma ray flashes from the Fermi gamma-ray burst monitor. *Journal of Geophysical Research*, 115, A07323. https://doi.org/10.1029/2009JA015242
 Celestin, S., Xu, W., & Pasko, V. P. (2012). Terrestrial gamma ray flashes with energies up to 100 MeV produced by nonequilibrium acceleration of electrons in lightning. *Journal of Geophysical Research*, 117, A05315. https://doi.org/10.1029/2012JA017535
- Connaughton, V., Briggs, M. S., Holzworth, R. H., Hutchins, M. L., Fishman, G. J., Wilson-Hodge, C. A., et al. (2010). Associations between Fermi gamma-ray burst monitor terrestrial gamma ray flashes and sferics from the world wide lightning location network. *Journal of Geophysical Research*, 115, A12307. https://doi.org/10.1029/2010JA015681
- Cummer, S. A., Briggs, M. S., Dwyer, J. R., Xiong, S., Connaughton, V., Fishman, G. J., et al. (2014). The source altitude, electric current, and intrinsic brightness of terrestrial gamma ray flashes. *Geophysical Research Letters*, 41, 8586–8593. https://doi.org/10.1002/2014GL062196 Cummer, S. A., Lu, G., Briggs, M. S., Connaughton, V., Xiong, S., Fishman, G. J., & Dwyer, J. R. (2011). The lightning-TGF relationship on microsecond timescales. *Geophysical Research Letters*, 38, L14810. https://doi.org/10.1029/2011GL048099
- Cummer, S. A., Zhai, Y., Hu, W., Smith, D. M., Lopez, L. I., & Stanley, M. A. (2005). Measurements and implications of the relationship between lightning and terrestrial gamma ray flashes. *Geophysical Research Letters*, 32, L08811. https://doi.org/10.1029/2005GL022778
 Dwyer, J. R. (2008). Source mechanisms of terrestrial gamma-ray flashes. *Journal of Geophysical Research*, 113, D10103. https://doi.org/10.1029/2007JD009248
- Dwyer, J. R., Rassoul, H. K., Al-Dayeh, M., Caraway, L., Wright, B., Chrest, A., et al. (2004). A ground level gamma-ray burst observed in association with rocket-triggered lightning. *Geophysical Research Letters*, 31, L05119. https://doi.org/10.1029/2003GL018771
- Dwyer, J. R., Schaal, M. M., Cramer, E., Arabshahi, S., Liu, N., Rassoul, H. K., et al. (2012). Observation of a gamma-ray flash at ground level in association with a cloud-to-ground lightning return stroke. *Journal of Geophysical Research*, 117, A10303. https://doi.org/10.1029/2012JA017810
- Fishman, G. J., Bhat, P. N., Mallozzi, R., Horack, J. M., Koshut, T., Kouveliotou, C., et al. (1994). Discovery of intense gamma-ray flashes of atmospheric origin. *Science*, 264(5163), 1313–1316. https://doi.org/10.1126/science.264.5163.1313
- Hare, B. M., Uman, M. A., Dwyer, J. R., Jordan, D. M., Biggerstaff, M. I., Caicedo, J. A., et al. (2016). Ground-level observation of a terrestrial gamma ray flash initiated by a triggered lightning. *Journal of Geophysical Research: Atmospheres*, 121, 6511–6533. https://doi.org/10.1002/2015JD024426

ZHANG ET AL. 10 of 12



Geophysical Research Letters

- Huang, A., Lu, G., Zhang, H., Liu, F., Fan, Y., Zhu, B., et al. (2018). Locating parent lightning strokes of sprites observed over a mesoscale convective system in Shandong province, China. Advances in Atmospheric Sciences, 35(11), 1396–1414. https://doi.org/10.1007/s00376-018-7306-4
- Leal, A. F. R., & Rakov, V. A. (2019). A study of the context in which compact intracloud discharges occur. Scientific Reports, 9, 12218. https://doi.org/10.1038/s41598-019-48680-6
- Li, X. B., Song, L. M., Li, X. F., Tan, Y., Yang, Y. J., & Ge, M. Y. (2018). In-orbit calibration status of the Insight-HXMT. *Proceedings of SPIE*, 10699, 069969. https://doi.org/10.1117/12.2315166
- Liu, F., Zhu, B., Lu, G., Qin, Z., Lei, J., Peng, K.-M., et al. (2018). Observations of blue discharges associated with negative narrow bipolar events in active deep convection. *Geophysical Research Letters*, 45, 2842–2851. https://doi.org/10.1002/2017GL076207
- Lu, G., Blakeslee, R. J., Li, J., Smith, D. M., Shao, X.-M., McCaul, E. W., et al. (2010). Lightning mapping observation of a terrestrial gamma-ray flash. *Geophysical Research Letters*, 37, L11806. https://doi.org/10.1029/2010GL043494
- Lu, G., Cummer, S. A., Li, J., Han, F., Smith, D. M., & Grefenstette, B. W. (2011). Characteristics of broadband lightning emissions associated with terrestrial gamma ray flashes. *Journal of Geophysical Research*, 116, A03316. https://doi.org/10.1029/2010JA016141
- Lu, G., Zhang, H., Cummer, S. A., Wang, Y., Lyu, F., Briggs, M., et al. (2019). A comparative study on the lightning sferics associated with terrestrial gamma-ray flashes observed in Americas and Asia. *Journal of Atmospheric and Solar-Terrestrial Physics*, 183, 67–75. https://doi.org/10.1016/j.jastp.2019.01.001
- Lyu, F., Cummer, S. A., Briggs, M., Marisaldi, M., Blakeslee, R. J., Bruning, E., et al. (2016). Ground detection of terrestrial gamma ray flashes from distant radio signals. *Geophysical Research Letters*, 43, 8728–8734. https://doi.org/10.1002/2016GL070154
- Lyu, F., Cummer, S. A., Krehbiel, P. R., Rison, W., Briggs, M. S., Cramer, E., et al. (2018). Very high frequency radio emissions associated with the production of terrestrial gamma-ray flashes. *Geophysical Research Letters*, 45, 2097–2105. https://doi.org/10.1002/2018GL077102
- Lyu, F., Cummer, S. A., & McTague, L. (2015). Insights into high peak current in-cloud lightning events during thunderstorms. *Geophysical Research Letters*, 42, 6836–6843. https://doi.org/10.1002/2015GL065047
- Mailyan, B. G., Xu, W., Celestin, S., Briggs, M. S., Dwyer, J. R., Cramer, E. S., et al. (2019). Analysis of individual terrestrial gamma-ray flashes with lightning leader models and fermi gamma-ray burst monitor data. *Journal of Geophysical Research: Space Physics*, 124, 7170–7183. https://doi.org/10.1029/2019JA026912
- Mallick, S., Rakov, V. A., Ngin, T., Gamerota, W. R., Pilkey, J. T., Hill, J. D., et al. (2014). Evaluation of the GLD360 performance characteristics using rocket-and-wire triggered lightning data. *Geophysical Research Letters*, 41, 3636–3642. https://doi.org/10.1002/2014GL059920
- Marisaldi, M., Fuschino, F., Labanti, C., Galli, M., Longo, F., Del Monte, E., et al. (2010). Detection of terrestrial gamma ray flashes up to 40 MeV by the AGILE satellite. *Journal of Geophysical Research*, 115, A00E13. https://doi.org/10.1029/2009JA014502
- Marshall, T., Stolzenburg, M., Karunarathne, S., Cummer, S., Lu, G., Betz, H.-D., et al. (2013). Initial breakdown pulses in intracloud lightning flashes and their relation to terrestrial gamma ray flashes. *Journal of Geophysical Research: Atmospheres*, 118, 10907–10925. https://doi.org/10.1002/jgrd.50866
- Nag, A., Rakov, V. A., Tsalikis, D., & Cramer, J. A. (2010). On phenomenology of compact intracloud lightning discharges. *Journal of Geophysical Research*, 115, D14115. https://doi.org/10.1029/2009JD012957
- Neubert, T., Østgaard, N., Reglero, V., Chanrion, O., Heumesser, M., Dimitriadou, K., et al. (2020). A terrestrial gamma-ray flash and ionospheric ultraviolet emissions powered by lightning. Science, 367, 183. https://doi.org/10.1126/science.aax3872
- Østgaard, N., Gjesteland, T., Carlson, B. E., Collier, A. B., Cummer, S. A., Lu, G., & Christian, H. J. (2013). Simultaneous observations of optical lightning and terrestrial gamma ray flash from space. *Geophysical Research Letters*, 40, 2423–2426. https://doi.org/10.1002/grl.50466
- Pu, Y., Cummer, S. A., Lyu, F., Briggs, M., Mailyan, B., Stanbro, M., & Roberts, O. (2019). Low frequency radio pulses produced by terrestrial gamma-ray flashes. *Geophysical Research Letters*, 46, 6990–6997. https://doi.org/10.1029/2019GL082743
- Sabri, M. H. M., Ahmad, M. R., Esa, M. R. M., Periannan, D., Lu, G., Zhang, H., et al. (2019). Initial electric field changes of lightning flashes in tropical thunderstorms and their relationship to the lightning initiation mechanism. *Atmospheric Research*, 226, 138–151. https://doi.org/10.1016/j.atmosres.2019.04.013
- Shao, X.-M., Hamlin, T., & Smith, D. M. (2010). A closer examination of terrestrial gamma-ray flash-related lightning processes. *Journal of Geophysical Research*, 115, A00E30. https://doi.org/10.1029/2009JA014835
- Smith, D. A., Heavner, M. J., Jacobson, A. R., Shao, X. M., Massey, R. S., Sheldon, R. J., & Wiens, K. C. (2004). A method for determining intracloud lightning and ionospheric heights from VLF/LF electric field records. *Radio Science*, 39, RS1010. https://doi.org/10.1029/2002RS002790
- Smith, D. M., Lopez, L. I., Lin, R. P., & Barrington-Leigh, C. P. (2005). Terrestrial Gamma-ray flashes observed up to 20 MeV. Science, 307, 1085–1088. https://doi.org/10.1126/science.1107466
- Stanley, M. A., Shao, X.-M., Smith, D. M., Lopez, L. I., Pongratz, M. B., Harlin, J. D., et al. (2006). A link between terrestrial gamma-ray flashes and intracloud lightning discharges. *Geophysical Research Letters*, 33, L06803. https://doi.org/10.1029/2005GL025537
- Tilles, J. N., Krehbiel, P. R., Stanley, M. A., Rison, W., Liu, N., Lyu, F., et al. (2020). Radio interferometer observations of an energetic incloud pulse reveal large currents generated by relativistic discharges. *Journal of Geophysical Research: Atmospheres*, 125, e2020JD032603. https://doi.org/10.1029/2020JD032603
- Tran, M. D., Rakov, V. A., Mallick, S., Dwyer, J. R., Nag, A., & Heckman, S. (2015). A terrestrial gamma-ray flash recorded at the Lightning Observatory in Gainesville, Florida. *Journal of Atmospheric and Solar-Terrestrial Physics*, 136, 86–93. https://doi.org/10.1016/j.jastp.2015.10.010
- Ursi, A., Marisaldi, M., Tavani, M., Casella, D., Sanò, P., & Dietrich, S. (2016). Detection of multiple terrestrial gamma-ray flashes from thunderstorm systems. *Journal of Geophysical Research: Space Physics*, 121, 11302–11315. https://doi.org/10.1002/2016JA023136
- Wu, T., Dong, W., Zhang, Y., Funaki, T., Yoshida, S., Morimoto, T., et al. (2012). Discharge height of lightning narrow bipolar events. *Journal of Geophysical Research*, 117, D05119. https://doi.org/10.1029/2011JD017054
- Wu, T., Takayanagi, Y., Yoshida, S., Funaki, T., Ushio, T., & Kawasaki, Z. (2013). Spatial relationship between lightning narrow bipolar events and parent thunderstorms as revealed by phased array radar. Geophysical Research Letters, 40, 618–623. https://doi.org/10.1002/ grl.50112
- Wu, T., Yoshida, S., Ushio, T., Kawasaki, Z., & Wang, D. (2014). Lightning-initiator type of narrow bipolar events and their subsequent pulse trains. *Journal of Geophysical Research: Atmospheres*, 119, 7425–7438. https://doi.org/10.1002/2014JD021842
- Xu, W., Celestin, S., & Pasko, V. P. (2012). Source altitudes of terrestrial gamma-ray flashes produced by lightning leaders. *Geophysical Research Letters*, 39, L08801. https://doi.org/10.1029/2012GL051351
- Xu, W., Celestin, S., & Pasko, V. P. (2015). Optical emissions associated with energetic electrons produced by stepping leaders in cloud-to-ground lightning discharges. Geophysical Research Letters, 42, 5610–5616. https://doi.org/10.1002/2015GL064419

ZHANG ET AL. 11 of 12



10.1029/2020GL092160



- Zhang, H., Lu, G., Lyu, F., Ahmad, M. R., Qie, X., Cummer, S. A., et al. (2020a). First measurements of low-frequency sferics associated with terrestrial gamma-ray flashes produced by equatorial thunderstorms. *Geophysical Research Letters*, 47, e2020GL089005. https://doi.org/10.1029/2020GL089005
- Zhang, H., Lu, G., Qie, X., Jiang, R., Fan, Y., Tian, Y., et al. (2016). Locating narrow bipolar events with single-station measurement of low-frequency magnetic fields. *Journal of Atmospheric and Solar-Terrestrial Physics*, 143–144, 88–101. https://doi.org/10.1016/j. jastp.2016.03.009
- Zhang, S., Li, T., Lu, F., Song, L., Xu, Y., Liu, C., et al. (2020b). Overview to the Hard X-ray Modulation Telescope (*Insight*-HXMT) Satellite. Science China Physics, Mechanics and Astronomy, 63, 249502. https://doi.org/10.1007/s11433-019-1432-6

ZHANG ET AL. 12 of 12